



Impact Factor: 0.962

Source: 2014 Journal Citation Reports®  
(Thomson Reuters, 2015)**Transactions of the Institute of Measurement and Control**

tim.sagepub.com

Published online before print June 30, 2015, doi: 10.1177/0142331215590470

Transactions of the Institute of Measurement and Control June 30, 2015  
0142331215590470A [more recent](#) version of this article was published on [02-15-2016]

## Design and simulation of a novel indoor mobile robot localization method using a light-emitting diode positioning system

Ngoc-Tan Nguyen<sup>1</sup>Anan Suebsomran<sup>2</sup>Keattisak Sripimanwat<sup>3</sup>Nam-Hoang Nguyen<sup>1</sup><sup>1</sup>Faculty of Electronics and Telecommunications, University of Engineering and Technology, Vietnam National University, Vietnam<sup>2</sup>Industrial Robot Research and Development Center, King Mongkut's University of Technology North Bangkok, Thailand<sup>3</sup>National Electronics and Computer Technology Center (NECTEC), NSTDA, ThailandAnan Suebsomran, Industrial Robot Research and Development Center, King Mongkut's University of Technology North Bangkok, 1518 Pracharat 1 Rd, Bangsue, Bangkok 10800, Thailand. Email: [asr@kmutnb.ac.th](mailto:asr@kmutnb.ac.th)**Abstract**

A key problem of mobile robots is that of the positioning capability in order to detect their locations in the operating environment. A promising technology used in indoor localization recently is Visible Light Communication (VLC). In this paper, an integrated Angle of Arrival-Received Signal Strength (AOA-RSS) localization method using the VLC, which could get high accuracy with simple hardware, is proposed. In addition, the Extended Kalman Filter (EKF) and Particle Filter (PF) algorithms are combined with the proposed AOA-RSS localization method in order to achieve higher accuracy of the mobile robot positioning. By computer simulation, the performance of the proposed AOA-RSS localization method combined with the EKF and PF algorithms are compared. The combination scheme outperforms the individual VLC localization with small error approximation of a few centimetres.

[Visible Light Communication](#)   [indoor localization](#)   [Extended Kalman Filter](#)  
[Particle Filter](#)

**Introduction**

White LEDs are expecting to become the next generation of light sources. Incandescent and fluorescent lamps have been gradually replaced by white LEDs because of their advantageous characteristics, such as long life expectancy, high brightness, ability of dimming and lower power consumption for illumination purpose (Komine and Nakagawa, 2004). Moreover, the LEDs have the ability of data transmission because they can be modulated at a fairly high rate (Grubor et al., 2008; Komine and Nakagawa, 2004). For these benefits, they are used as a primary element in the Visible Light Communication (VLC) system, which is attracting many researchers working on its applications, both illumination and data transmission.

Throughout the past decade, the appearance of mobile robots has become very popular in all aspects of society. Mobile robots appear in household appliances such as in vacuum cleaning machines and home assistance. They can also be found in public, industrial and military fields, such as in guidance robots and material transport robots. Mobile robots have the capability to move around their workspace and reach the desired target positions. In order to perform this capability, mobile robots need to know their positions in the environment. Although the Global Positioning System (GPS) works well in outdoor environment, for small and covered indoor environments such as buildings, factories, museum, etc., the GPS provides location information with poor accuracy, and even sometimes is unavailable.

To deal with this challenge, a number of techniques for indoor localization have been

proposed and developed based on using video cameras, laser sensors, ultrasonic sensors and radio frequency/wireless identification sensors ([Achour and Djekoune, 2012](#); [Choi et al., 2012a](#); [Hsieh et al., 2009](#); [Jia et al., 2012](#); [Nagai et al., 2013](#)). Recently, localization using VLC technology with certain benefits has become a promising technology to replace those sensors. There is an increasing number of published articles that present a variety of indoor localization methods based on the VLC, such as Time of Arrival (TOA) ([Cheung et al., 2004](#); [Wang et al., 2013](#)), Time Difference of Arrival (TDOA) ([Choi et al., 2012b](#); [Gustafsson, 2003](#); [Xu et al., 2011](#)), Received Signal Strength (RSS) ([Jung et al., 2013](#)) and Angle of Arrival (AOA) ([Lee and Jung, 2012](#)). Due to the short time of arrival light and requiring time synchronization between transmitters and receivers, the TOA and TDOA methods are not feasible for indoor localization based on the VLC. Meanwhile, the RSS method does not achieve high accuracy when it is implemented in environments having a poor path loss model. Although the AOA method achieves higher accuracy than the others, it often requires a complex hardware and is only capable of one-dimensional positioning ([Lee and Jung, 2012](#)). Therefore, an integration of the AOA and RSS methods proposed in this paper is a highly promising alternative for other individuals because higher accuracy and less complexity of implementation could be achieved.

Only the measurement from VLC sensors might provide a noisy observation for the estimation of the mobile robot's location. Therefore, more highly accurate robots need a solution to combine the observations from both the sensors and robotic model. The term "location estimator" is used for probabilistic estimators, which are used on mobile robots to carry out the above combination. To date, there have been a number of location estimators proposed and studied. One traditional estimator subject to Gaussian noise for linear systems is the Kalman Filter (KF) ([Kailath et al., 2000](#); [Negenborn, 2003](#); [Simon, 2006](#); [Thrun et al., 2005](#)) and for non-linear systems is the Extended Kalman Filter (EKF) ([Angel and Rosa, 2009](#); [Duong et al., 2013](#); [Kailath et al., 2000](#); [Larsen et al., 1999](#); [Negenborn, 2003](#); [Pillonetto et al., 2012](#); [Santana et al., 2008](#); [Siegwart et al., 2004](#); [Simon, 2006](#); [Thrun et al., 2005](#)). However, because the EKF relies on a fixed functional form of a *posterior*, it is difficult to tune and often gives unreliable values. An alternative for approximating the system using linearization is the Particle Filter (PF) ([Angel and Rosa, 2009](#); [Armingol et al., 2012](#); [Cen et al., 2009](#); [Fox et al., 2001](#); [Rstic et al., 2004](#); [Simon, 2006](#); [Thrun, 2002](#); [Thrun et al., 2005](#); [Woo et al., 2006](#)). In this paper, the combinations of the proposed AOA-RSS localization method with the EKF and the PF in order to enhance accuracy in positioning a mobile robot are presented. This work is done by computer simulation. The expectation is that the lowest estimated error could be achieved with the combination scheme and the mobile robot could be controlled to follow its path precisely by the estimation techniques as the objective.

This paper is organized as follows. Two individual VLC localization methods with low accuracy are briefly described in previous works in the second section. An integrated AOA-RSS localization method is then proposed for high accurate positioning in the third section. The combination schemes between the proposed localization method with the EKF and the PF estimators for our proposed system are described and discussed in the fourth and fifth sections, respectively. Our simulation results of the combination schemes will be shown in the sixth section. Conclusions are given in the last section.

## Previous works

As an effective alternative for traditional localization technologies and sensors, the use of the VLC system and light-emitting diode (LED)-based devices to localize the mobile robot's position has become more popular in practice because of its benefits, especially both illumination and signal transmission. A number of VLC localization methods using geometric properties of triangles to estimate the target position have been proposed so far. Those are called triangulation methods and will be briefly described as follows.

### Received Signal Strength method

In order to perform any VLC localization method based on the intensity of the received optical signal power, a VLC channel model given by [Kominé and Nakagawa \(2004\)](#) has to be utilized. The position of the mobile robot is estimated by measuring this power at the photodiodes (PDs).

The channel direct current (DC) gain of the VLC channel is given as

$$H(0) = \begin{cases} \frac{(m+1)A}{2\pi D_d^2} \cos^m(\phi) T_s(\psi) g_s(\psi) \cos(\psi), & 0 \leq \psi \leq \psi_c \\ 0, & \psi \geq \psi_c \end{cases} \quad (1)$$

where  $A$  is the physical area of a PD detector;  $D_d$  is the distance between a transmitter and a receiver; and  $\psi$  and  $\phi$  are the angle of incidence and irradiance, respectively.  $T_s(\psi)$  is the gain of an optical filter, while  $\cos^m(\phi)$  and  $\cos(\psi)$  denote the LED and PD sensitivity.  $g(\psi)$  is the gain of an optical concentrator. The power  $P_r$  then becomes

$$P_r = H(0)P_t = \frac{(m+1)A}{2\pi D_d^2} \cos^m(\phi) T_s(\psi) g_s(\psi) \cos(\psi) P_t \quad (2)$$

As shown in [Figure 1](#), the transceivers are located on the horizontal planes. Hence, the incidence angle  $\psi$  is equal to the irradiance angle  $\phi$ :

$$P_r(D_d) = \frac{(m+1)Ah^{m+1}}{2\pi D_d^{m+3}} T_s(\psi) g_s(\psi) P_t \quad (3)$$

where  $h$  is the height of the LED. [Equation \(3\)](#) indicates that the power  $P_r$  is a function of distance  $D_d$ . At least three transmitters are required to draw imaginary circles centred at their coordinates. Thus, the position of the mobile robot will be the intersection point of these circles. Nevertheless, the receiver output always contains a Gaussian noise  $N$  that is contributed by shot noise, thermal noise and inter-symbol interference ([Komine and Nakagawa, 2004](#)). It means that the imaginary circles do not intersect at a common point, but they create an overlapped area. Therefore, the mobile robot is located somewhere in that area. Its position is calculated by common estimators such as Cramér-Rao lower bound (CRLB), circular error probability (CEP) and least squares (LS) ([Cheung et al., 2004](#); [Choi et al., 2012b](#); [Wang et al., 2013](#)). This method can only provide accurate location information with low complexity of receivers in a pure line of sight (LOS) environment. Its accuracy will be decreased when the robot moves into a poor VLC area. Moreover, it also requires at least three transmitters to send data.

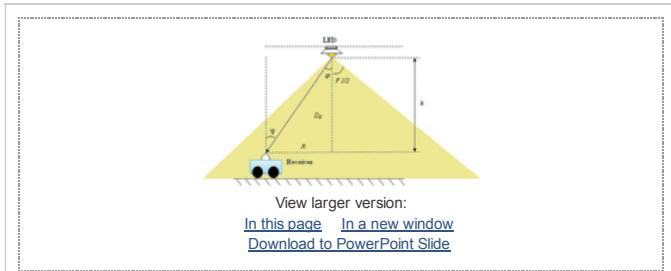


**Figure 1.**

System model of an optical wireless channel.

### Angle of Arrival method

The Angle of Arrival is defined as the angle between the propagation direction of an incident light wave and a reference direction, which is known as orientation. A model of the AOA method using a circular PD array is described by [Lee and Jung \(2012; Figure 2\)](#). The number of PDs in the circular PD array affects performance of the AOA method. The more PDs integrated are in the circular PD array, the lower estimated error can be achieved. [Figure 3](#) shows the system model location awareness. The angle of the  $i$ th PD is determined as follows, with  $K$  being the number of PDs:

$$\theta_i = \pi i / (K - 1) \quad (4)$$

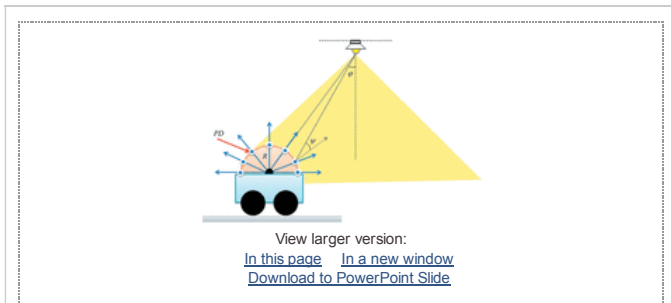
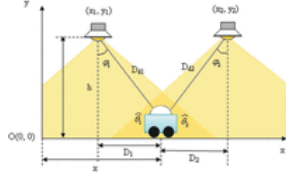


**Figure 2.**

System model of the Angle of Arrival method based on a circular PD array.

**Figure 3.**

The system model location awareness.



View larger version:  
[In this page](#) [In a new window](#)  
[Download to PowerPoint Slide](#)

To get higher estimation accuracy, the “truncated-weighting” method is proposed by [Lee and Jung \(2012\)](#) to calculate the estimated angles  $\hat{\theta}_1$  and  $\hat{\theta}_2$ . The x-axis position of the mobile robot is then estimated by taking an average of the distances  $D_1$  and  $D_2$  from the horizontal positions of LEDs to the robot ([Figure 3](#)).

The AOA achieves a number of significant benefits, such as well corresponding to the propagation environment LOS of VLC, getting higher accuracy compared to other methods by using an array of PDs. In addition, it does not need to sync time between the transmitter and the receiver. Nonetheless, the AOA has several drawbacks, such as requiring a complex hardware and providing only a one-dimensional position of the mobile robot. Moreover, the error of 33 cm with 17 PDs of the model in [Lee and Jung \(2012\)](#) is still quite high for indoor localization.

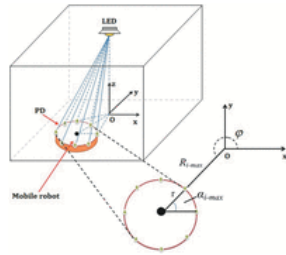
### Integrated AOA-RSS localization method

Several localization methods described in the previous section have a number of drawbacks when they are used individually. To overcome these drawbacks, a novel localization method integrating the AOA and RSS is proposed as follows.

#### System model

A flattened circle of PDs is utilized to measure received optical powers and determine the orientation of the mobile robot. Calculation of PD positions is executed based on the knowledge of the mobile robot's pose. The proposed system model is shown in [Figure 4](#). The angle of the  $i$ th PD is determined as follows, where  $\theta$  is the orientation of the mobile robot and  $K$  is the number of PDs mounted on the robot:

$$\alpha_i = \frac{2\pi(i-1)}{K} + \theta \quad (5)$$



View larger version:  
[In this page](#) [In a new window](#)  
[Download to PowerPoint Slide](#)

**Figure 4.**

System model of the integrated Angle of Arrival-Received Signal Strength localization method using an array of PDs .

#### System noise

As mentioned in the previous section, an optical wireless channel with Gaussian noises presented by [Komine et al. \(2004\)](#) is applied for all VLC-based localization methods in this paper. The real received power at the  $i$ th receiver's output is given as

$$\begin{aligned} P_{\text{signal}}(i) &= \mathbf{H}(0)\mathbf{P}_t + \mathbf{N}(i) \\ &= \mathbf{H}(0)\mathbf{P}_t = \frac{(m+1)Ah^{m+1}}{2\pi\sqrt{(R^2(i)+h^2)^{m+3}}} T_s(\psi)g_s(\psi)\mathbf{P}_t + \mathbf{N}(i) \end{aligned} \quad (6)$$

where  $\mathbf{N}(i)$  is the total covariance of Gaussian noises,  $\sigma_{\text{shot}}^2(i)$  and  $\mathbf{P}_{\text{ISI}}^2(i)$  are the variance of shot noise and the inter-symbol interference (ISI) power at the  $i$ th PD,

respectively,  $\sigma_{\text{thermal}}^2$  is the thermal variance and

$$N(i) = \sigma_{\text{shot}}^2(i) + \sigma_{\text{thermal}}^2 + \gamma^2 P_{\text{rISI}}^2(i) \quad (7)$$

System parameters for the calculation of the channel DC gain and Gaussian noises are shown in [Table 1](#).

<p>View this table:  <a href="#">In this window</a> <a href="#">In a new window</a>  <a href="#">Download to PowerPoint Slide</a></p>
<p><b>Table 1.</b> System parameters.</p>

### Operation of the integrated AOA-RSS method

At the first step, the integrated AOA-RSS determines the direction of the mobile robot compared with a transmitter's position to which it is connecting, based on the special configuration of the PD array. From received signal powers at the receiver output, the mobile robot detects the PD that received the maximum signal power from the transmitter. This means the PD that is closest to the transmitter. The mobile robot selects the angle of this PD ( $\alpha_{i-\text{max}}, i-\text{max} = \max P_{r\_signal}(i)$ ) as the angle between the heading direction of the mobile robot and the horizontal distance between the LED and the centre of the mobile robot ([Figure 4](#)).

In the next step, the integrated AOA-RSS estimates the location of the mobile robot's centre based on the angle  $\alpha_{i-\text{max}}$ . The horizontal distance between the LED and the PD having maximum received power  $R_{i-\text{max}}$  is approximated by [Equation \(6\)](#). The global coordinate of the mobile robot ( $C_x, C_y$ ) can be then calculated as follows.

- Case 1: When the mobile robot is at the position where it satisfies the condition  $R_{i-\text{max}} \geq r$ :

$$\begin{cases} C_x = x_{LED} + (r + R_{i-\text{max}}) \cos(\varphi) \\ C_y = y_{LED} + (r + R_{i-\text{max}}) \sin(\varphi) \end{cases} \quad (8)$$

- Case 2: When the mobile robot is at the position where satisfies the condition  $R_{i-\text{max}} < r$ :

$$\begin{cases} C_x = x_{LED} + (r - R_{i-\text{max}}) \cos(\varphi) \\ C_y = y_{LED} + (r - R_{i-\text{max}}) \sin(\varphi) \end{cases} \quad (9)$$

where  $\varphi$  is the angle between the horizontal distance from the LED to the PD that received the maximum signal power and the horizontal line ([Figure 4](#)). It can easily be calculated from the angle of the heading direction of the mobile robot compared with the LED  $\alpha_{i-\text{max}}$ . In addition, ( $x_{LED}, y_{LED}$ ) is the global coordinate of the LED.

For most common types of indoor environments, such as offices, museums, libraries, hospitals and factories where there are long corridors with a usual width of 2 m, LEDs with equal distances from each other of 1.5 m are aligned horizontally and vertically. The coverage of each LED has a radius of 1.732 m, which is calculated from the parameters in [Table 1](#). With this setup, the mobile robot is always under the coverage of at least two LEDs. Therefore, the accuracy of the integrated AOA-RSS method is then enhanced because of receiving location information from at least two transmitters.

The number of PDs and Gaussian noises are two key parameters that directly affect the accuracy of the integrated AOA-RSS. Its estimated error is alleviated according to increasing the number of PDs mounted on the mobile robot. The second parameter that distorts the received signal power at the receiver output is Gaussian noises involving the shot noise, thermal noise and inter-symbol interference. Although this method suffers these errors it can get higher accuracy than the individual methods. With 16 PDs mounted on the robot, this method has the error less than 20 cm, which is better than the model in [Lee and Jung \(2012\)](#).

### Location estimators

Although the proposed AOA-RSS localization achieves a high accuracy with the simple hardware, there still exist some shortcomings, such as increasing the number of PDs is limited due to hardware installation and the capability to distinguish levels of received signal power at PDs. Therefore, two popular location estimation techniques, the EKF and PF, are combined with the proposed AOA-RSS localization in order to achieve more accuracy in positioning indoor mobile robots in this section.

### The system model of the mobile robot: kinematic configuration

The effect of control actions on the robot's configuration is expressed by kinematic equations. The configuration is commonly described by its six variables, three-dimensional Cartesian coordinates and its three Euler angles (roll, pitch and yaw) relative to an external coordinate frame (Thrun et al., 2005). For most mobile robot models operating in the planar environment, there are only three variables to denote the two-dimensional planar coordinates of the mobile robot in the global coordinate frame and its angular orientation. These variables are called the mobile robot's pose that is described by the state vector  $\mathbf{x}_k = (x_k, y_k, \theta_k)$  (Figure 5(a)). The mobile robot's pose can be easily calculated by a classic method called the Odometry. Sensors such as optical encoders are used by the Odometry method to measure the rotation of the robot's wheels (Santana et al., 2008).

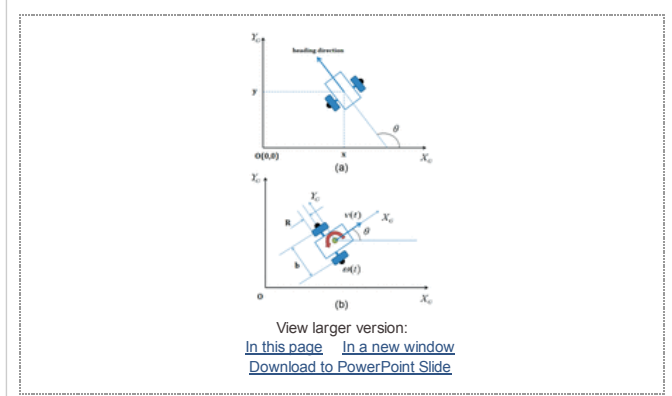


**Figure 5.**

(a) Kinematic configuration: the pose of the mobile robot in a global coordinate system. (b) Kinematic configuration: system model of the two-wheeled mobile robot.

Figure 5(b) shows the model of our two-wheeled mobile robot, which has the local coordinate relative to the robot chassis ( $X_R, Y_R$ ) in the global coordinate system ( $X_G, Y_G$ ). The radius of the wheels and the distance between them are denoted by  $a$  and  $b$ , respectively.

Movement time of the mobile robot is sampled into period  $\Delta t$  that is small enough. Hence, the linear displacement of the robot's centre  $\Delta s$  and the robot's orientation angle  $\Delta \theta$  in each sampling period  $\Delta t$  are estimated from linear travelled distances of the left wheel  $\Delta s_L$  and the right wheel  $\Delta s_R$ :

$$\Delta s = (\Delta s_R + \Delta s_L)/2; \Delta \theta = (\Delta s_R - \Delta s_L)/b \quad (10)$$

where linear travelled distances  $\Delta s_L$  and  $\Delta s_R$  are calculated from rotational speeds of the left wheel  $\omega_L$  and right wheel  $\omega_R$  after each sampling period  $\Delta t$ , respectively:

$$\Delta s_L = \Delta t R \omega_L; \Delta s_R = \Delta t R \omega_R \quad (11)$$

The mobile robot's pose at time  $k+1$  in the global coordinate frame is calculated according to the mobile robot's pose, the linear displacement of the robot's centre  $\Delta s$  and the robot's orientation angle  $\Delta \theta$  at time  $k$ :

$$\begin{bmatrix} x_{k+1} \\ y_{k+1} \\ \theta_{k+1} \end{bmatrix} = \begin{bmatrix} x_k \\ y_k \\ \theta_k \end{bmatrix} + \begin{bmatrix} \Delta s_k \cos(\theta_k + \Delta \theta_k/2) \\ \Delta s_k \sin(\theta_k + \Delta \theta_k/2) \\ \Delta \theta_k \end{bmatrix} \quad (12)$$

Unfortunately, the kinematic equation (12) is not really accurate in real systems because of unavoidable errors that come from both of the imperfectness of the robot, for instance, deformation of the wheel, limited encoder resolution, and the environment, such as wheel-slippage and unequal floors. These errors can break the stability of the system due to their accumulative characteristic. Therefore, real systems need an appropriate compensator to alleviate unavoidable errors (Duong et al., 2013).

An assumption is here that the next state probability and the measurement probabilities are governed by non-linear functions  $f$  and  $h$ , respectively:

$$\mathbf{x}_{k+1} = f(\mathbf{x}_k, \mathbf{u}_k, \mathbf{w}_k) \quad (13)$$

$$\mathbf{z}_{k+1} = h(\mathbf{x}_k, \mathbf{v}_k) \quad (14)$$

where  $f$  is expressed in [Equation \(12\)](#) and  $h$  is measurements that consist of the integrated AOA-RSS localization measurement and Gyro sensor measurement determining the rotated angle of the mobile robot. The random variables  $\mathbf{w}_k$  and  $\mathbf{v}_k$  represent the process of the mobile robot and measurement noise, respectively. They are assumed with properties involved to be independent of each other, white and with normal probability distributions:  $\mathbf{w}_k \sim N(0, \mathbf{Q}_k)$ ,  $\mathbf{v}_k \sim N(0, \mathbf{R}_k)$ ,  $E[\mathbf{w}_k, \mathbf{v}_k^T] = 0$  ([Larsen et al., 1999](#)).

### The Extended Kalman Filter

The EKF is an extension of the famous KF, which is in fact more efficient than the Markov localization estimator because of key simplification. The basic KF utilizes the linear system and linear measurement models to address the problem of estimating the state of a noisy system ([Negenborn, 2003](#)). Nevertheless, a system with the linear state transition and linear measurement added Gaussian noise are rarely fulfilled in practice. For example, a mobile robot that moves with constant translational and rotational velocity typically moves on a circular trajectory, which cannot be described by linear next state transitions ([Thrun et al., 2005](#)). Therefore, the improvement in the EKF is linearizing the linear state transition and linear measurement to overcome restriction of the KF.

The whole EKF algorithm is represented in [Table 2](#), where  $\hat{\mathbf{x}}_{k+1}^-$ ,  $\hat{\mathbf{x}}_{k+1}$  are the *priori* and *posterior* state estimates at step  $k+1$ , respectively;  $\mathbf{P}_{k+1}^-$  and  $\mathbf{P}_{k+1}$  denote the covariance matrixes of the state errors in prediction and correction stages, respectively;  $\mathbf{A}_{k+1}$  and  $\mathbf{H}_{k+1}$  are the Jacobian matrixes of partial derivatives of  $f$  and  $h$  functions.  $\mathbf{W}_{k+1}$  is the Jacobian matrix of partial derivatives of  $f$  to control vector  $\mathbf{w}(\Delta s_R, \Delta s_L)$ .  $\mathbf{Q}_{k+1}$  is the input-noise covariance matrix, which depends on the travelled distances by wheels  $\Delta s_R$ ,  $\Delta s_L$  and error constants representing the nondeterministic parameters of the motors and the wheel-floor interaction  $k_R$ ,  $k_L$  ([Siegwart et al., 2004](#)):

$$\mathbf{Q}_k = \begin{bmatrix} k_R |\Delta s_R| & 0 \\ 0 & k_L |\Delta s_L| \end{bmatrix} \quad (15)$$

View this table:  
[In this window](#) [In a new window](#)  
[Download to PowerPoint Slide](#)

**Table 2.**

The Extended Kalman Filter algorithm.

In addition,  $\mathbf{K}_{k+1}$  is the Kalman gain;  $\mathbf{z}_{k+1}$  is the measurement of the mobile robot's pose from the proposed AOA-RSS localization method and Gyro sensor at time  $k+1$ .  $\mathbf{R}_{k+1}$  is the covariance matrix of the Gaussian noise of the measurement  $\mathbf{z}_k$ :

$$\mathbf{R}_{k+1} = \begin{bmatrix} \text{var}(x_{k+1}|_{VLC}) & 0 & 0 \\ 0 & \text{var}(y_{k+1}|_{VLC}) & 0 \\ 0 & 0 & \text{var}(\theta_{k+1}|_{Gyro}) \end{bmatrix} \quad (16)$$

The noise variance of the proposed AOA-RSS localization method is 0.0036. The error of the Gyro sensor is 3 degrees, corresponding to the noise variance of 0.0028 in radians, which is achieved from the manufacturer's specification.

### The Particle Filter

The PF has become an attractive non-linear state estimator to deal with the problem of mobile robot localization because of the dramatic growth of computational power. Actually, the PF is preferred over the KF because of several key advantages in robotics. The most significant advantage is that the PF can be applied to a large number of probability distributions, in contrast to the KF, which is used widely in problems using normal distribution ([Fox et al., 2001](#)). Moreover, the PFs also act as any-time filters because they do not require a fixed computational time, instead of the increase of their accuracy according to the computational resources ([Thrun, 2002](#)). Finally, whilst the KF is difficult to tune, the PF is remarkably easy to implement because linearizing non-linear mobile robot models are not required ([Fox et al., 2001](#); [Simon, 2006](#); [Thrun, 2002](#)).

All steps of the PF algorithm are listed in [Table 3](#), where  $N$  is the number of particles. The trade-off between computational effort and estimation accuracy is adjusted by choosing the parameter  $N$  of the user.  $\mathbf{X}_k^-$  is a set of priori particles at time  $k$ .  $\mathbf{Q}$  is a set of likelihoods corresponding to the set of priori  $\mathbf{X}_k^- = \{\mathbf{x}_{k,i}^-\} (i=1, 2, \dots, N)$  after we receive the measurement  $\mathbf{z}_k$  of the mobile robot's pose from the proposed AOA-RSS localization method and Gyro sensor at time  $k$ . Note that the relative likelihoods  $\mathbf{q}_i$  are

then normalized to ensure that the sum of all weights is equal to one.  $\mathbf{X}_k^+$  is a set of posterior particles that are set equal to the priori particles  $\mathbf{x}_{k,j}^-$  in step 4. Index  $j$  of the priori  $\mathbf{x}_{k,j}^-$  is detected by using a direct approach presented by [Rstic et al. \(2004\)](#).

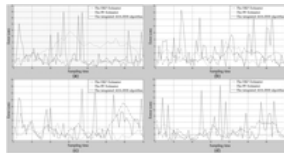
View this table:  
[In this window](#) [In a new window](#)  
[Download to PowerPoint Slide](#)

**Table 3.**  
The Particle Filter algorithm.

### Simulation results and performance analysis

The goal of the simulation implementation is to evaluate the performance of location estimators discussed early in this paper by varying certain parameters. From these evaluations, performance of the combination scheme between the location estimators EKF and PF with the proposed AOA-RSS localization method are compared to choose the best one satisfying the mobile robot model. A simulation scenario is that the mobile robot is controlled to move on the specified path connecting two global points (1, 1) and (8, 1).

The integrated AOA-RSS localization is presented with performance depending on the number of mounted PDs. In this paper, 16 mounted PDs are utilized to achieve errors approximating 20 cm. These errors are fairly high for indoor localization applications. Therefore, the EKF and PF estimators are applied to enhance performance of the proposed AOA-RSS localization. [Figures 6\(a\)–\(d\)](#) show performance comparison of the combination schemes and the integrated AOA-RSS method. The line dotted with asterisks and the line dotted without asterisks denote errors of the combination schemes with the EKF and PF algorithms, respectively, while the solid line denotes error of the integrated AOA-RSS method. Four simulation cases corresponding to the numbers of particles  $N = 5, 30, 50$  and  $100$ , which are used in the combination scheme with the PF, are shown in [Figures 6\(a\)–\(d\)](#). It can be clearly seen from these figures that the accuracy of combination schemes is always greater than the integrated AOA-RSS method. In the worst estimation case of the PF algorithm (Case 1), the average error of this combination scheme with five particles is still smaller than the integrated AOA-RSS method in [Figure 6\(a\)](#). However, the accuracy of the scheme with the PF algorithm is very poor compared with the EKF algorithm. In this case, the error of the scheme with the PF estimator peaks at 11.5 cm, whereas the maximum error of the scheme with the EKF estimator is only 4.5 cm. As is highlighted in [Figure 6\(b\)](#) (Case 2), the PF algorithm with the number of particles  $N = 30$  achieves accuracy similar to the EKF algorithm of about 8 cm. When the number of particles is greater than 30, performance of the scheme with the PF becomes better than the EKF with maximum estimation error approximately 5 cm as shown in [Figures 6\(c\) and \(d\)](#).



View larger version:  
[In this page](#) [In a new window](#)  
[Download to PowerPoint Slide](#)

**Figure 6.**  
 (a) Accuracy comparison of combination schemes with the Extended Kalman Filter (EKF) and Particle Filter (PF) estimators. Case 1:  $N = 5$ . (b) Accuracy comparison of combination schemes with the EKF and PF estimators. Case 2:  $N = 30$ . (c) Accuracy comparison of combination schemes with the EKF and PF estimators. Case 3:  $N = 50$ . (d) Accuracy comparison of combination schemes with the EKF and PF estimators. Case 4:  $N = 100$ .

As discussed previously, unavoidable errors appeared in the mobile robot system, making the movement of the mobile robot between two points in a real environment difficultly. Therefore, estimators are not only applied to decrease the error of the integrated AOA-RSS localization method as estimators, but also play a role as compensators to alleviate the accumulative errors that appear in moving of the mobile robot on the specified path. [Figures 7\(a\)–\(d\)](#) show the operation of the EKF and PF compensators in controlling the mobile robot on the specified path. It can be clearly seen from these figures that the mobile robot is deviated quite far away from the desired path due to accumulative errors in the absence of any compensator. When compensators are applied, the mobile robot always approaches its path. These compensators fight against accumulative errors that appeared in moving of the mobile

robot by recalculating control vector  $\mathbf{u}$  after each period time  $\Delta t$ . The control vector  $\mathbf{u}$  is calculated to adjust the orientation of the mobile robot. In other words, the control vector  $\mathbf{u}$  alleviates accumulative errors. This ensures that the mobile robot always reaches the target point. [Figures 6\(a\)–\(d\)](#) show the performance of the EKF and PF estimators in the combination schemes corresponding to four simulation cases in [Figures 7\(a\)–\(d\)](#), respectively.

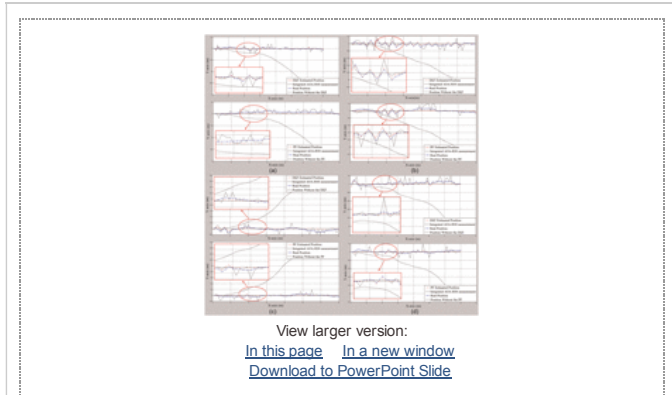


**Figure 7.**

(a) Operation of the Extended Kalman Filter (EKF) and Particle Filter (PF) compensators. Case 1:  $N = 5$ . (b) Operation of the EKF and PF compensators. Case 2:  $N = 30$ . (c) Operation of the EKF and PF compensators. Case 3:  $N = 50$ . (d) Operation of the EKF and PF compensators. Case 4:  $N = 100$ .

## Conclusions

In this paper, we presented indoor localization methods based on the VLCs. We proposed the integrated AOA-RSS localization method, which combines the AOA and RSS methods to take the benefits of both. This method achieves high accuracy of approximately 20 cm compared to other methods. In order to improve the accuracy of the VLC localization for indoor applications, combination schemes of the VLC localization measurement and estimators consisting of the EKF and the PF are then also presented. Evaluation by simulations proves that the combination schemes have achieved higher accuracy than the integrated AOA-RSS localization method by approximately a few centimetres. The Main result of this paper is then comparing the performance of the combination schemes with the EKF and PF estimators for trade-off depending on computational power. Moreover, the simulation results also mention that the EKF and PF work well in the role of compensators to alleviate accumulative errors of the system when the mobile robot moves on the specified path.

## Article Notes

**Conflicting of interest** The authors declare that there is no conflict of interest.

**Funding** This work was supported by the King Mongkut's University of Technology North Bangkok, Bangkok, Thailand (contract no. KMUTNB-GOV-58-60) and Vietnam National University (VNU), Hanoi, Vietnam.

## References

- Achour K, Diekouni A (2012) Localization and guidance with an embarked camera on a mobile robot. *Advanced Robotics Journal* 16(1): 87–102. [Google Scholar](#)
- Annel M, Rosa F (2009) Experimental comparison of Extended Kalman and Particle Filter in mobile robotic localization. In: *the CFRMA'09 conference on electronics robotics and automotive mechanics*, Cuernavaca, pp.157–162. [Google Scholar](#)
- Amingal JM, Escalera A, Moreno J, et al (2012) Mobile robot localization using a non-linear evolutionary filter. *Advanced Robotics Journal* 16(7): 629–652. [Google Scholar](#)
- Can G, Matsuhira N, Hirakawa J, et al (2009) New entropy-based adaptive particle filter for mobile robot localization. *Advanced Robotics Journal* 23(12–13): 1761–1778. [CrossRef](#) [Google Scholar](#)
- Cheung KW, So HC, Ma WK, et al (2004) Least squares algorithms for time-of-arrival-based mobile location. *IEE Transactions on Signal Processing* 52(4): 1121–1130. [CrossRef](#) [Google Scholar](#)
- Choi M, Choi J, Chung WK (2012a) Correlation-based scan matching using ultrasonic sensors for EKF localization. *Advanced Robotics Journal* 26(13): 1495–1519. [CrossRef](#) [Google Scholar](#)
- Choi YH, Park IH, Kim YH, et al. (2012b) Novel LBS Technique based on visible light

communications. In: *the 2012 IEEE international conference on consumer electronics*, Las Vegas, pp.576–577. [Google Scholar](#)

Duong PM, Van NTT, Hoang TT, et al. (2013) Localization of networked robot systems subject to random delay and packet loss. In: *the IEEE/ASME international conference on advanced intelligent mechatronics*, Wollongong, pp.1442–1447. [Google Scholar](#)

Fox D, Thrun S, Burdard W, et al. (2001) Particle filters for mobile robot localization. Available at: <http://citeseerx.ist.nyu.edu/viewdoc/summary?doi=10.1.1.1.9914> (accessed 10 August 2014). [Google Scholar](#)

Gruhn J, Randel S, Langer K, et al. (2008) Broadband information broadcasting using LED-based interior lighting. *Lightwave Technology Journal* 26(24): 3883–3892. [CrossRef](#) [Google Scholar](#)

Guetafesson F. (2003) Positioning using time difference of arrival measurements. In: *the IEEE international conference on acoustics, speech and signal proceedings*, Hong Kong, vol. 6, pp.553–556. [Google Scholar](#)

Hsieh CH, Wang MI, Kao LW, et al. (2009) Mobile robot localization and path planning using an omnidirectional camera and infrared sensors. In: *the 2009 IEEE international conference on systems, man, and cybernetics*, Texas, pp.1947–1952. [Google Scholar](#)

Jia S, Sheng J, Shang F, et al. (2012) Robot localization in indoor environments using radio frequency identification technology and stereo vision. *Advanced Robotics Journal* 22(2–3): 279–297. [Google Scholar](#)

Jung SY, Choi CK, Han SH, et al. (2013) Received signal strength ratio based optical wireless indoor localization using light emitting diodes for illumination. In: *the IEEE international conference on consumer electronics*, Las Vegas, pp.63–64. [Google Scholar](#)

Kailath T, Saeed A, Hassibi B (2000) *Linear Estimation*. NJ: Prentice Hall publisher. [Google Scholar](#)

Komine T, Nakanawa M (2004) Fundamental analysis for visible-light communication system using LED lights. *IEEE Transactions on Consumer Electronics* 50(1): 100–107. [CrossRef](#) [Google Scholar](#)

Larsen TD, Hansen KL, Andersen NA, et al. (1999) Design of Kalman filters for mobile robot: evaluation of kinematic and odometric approach. In: *the 1999 IEEE international conference on control applications*, Kohala Coast, vol.2, pp.1021–1026. [Google Scholar](#)

Lee SS, Jung SY (2012) Location awareness using angle-of-arrival based circular-PD-array for visible light communication. In: *the 18th Asia-Pacific conference on communications*, Jeju, Korea, pp.480–485. [Google Scholar](#)

Nagai I, Nanatani K, Yamauchi G, et al. (2013) Positioning device for outdoor mobile robots using optical sensors and lasers. *Advanced Robotics Journal* 27(15): 1147–1160. [CrossRef](#) [Google Scholar](#)

Nenchev R (2003) *Robot Localization and Kalman filters on finding your position in a noisy world*. Master's Thesis, Utrecht University, Utrecht. [Google Scholar](#)

Pillonetto G, Eric G, Carini S (2012) Online estimation of covariance parameters using extended Kalman filtering and application to robot localization. *Advanced Robotics Journal* 26(18): 2169–2188. [CrossRef](#) [Google Scholar](#)

Potter R, Anilampalam S, Gordon N (2004) *Beyond the Kalman Filter: Particle Filters for Tracking Applications*. Norwood, MA: Artech House Publisher. [Google Scholar](#)

Santana AM, Sousa DAS, Brito RS, et al. (2008) Localization of a mobile robot based in odometry and natural landmarks using Extended Kalman Filter. In: *ICINCO-RA 2*, INSTICC Press, pp.187–193. [Google Scholar](#)

Siegwart R, Nourbakhsh IR, Scaramuzza D (2004) *Introduction to Autonomous Mobile Robot*. Cambridge, MA: MIT Press publisher. [Google Scholar](#)

Simon D (2006) *Optimal State Estimation: Kalman, H-infinity and Nonlinear Approaches*. Hoboken, NJ: John Wiley & Sons, Inc. [Google Scholar](#)

Thrun S (2002) Particle filters in robotics. In: *the eighteenth conference on uncertainty in artificial intelligence*, San Francisco, pp.511–518. [Google Scholar](#)

Thrun S, Burdard W, Fox D (2005) *Probabilistic Robotics*. Cambridge, MA: MIT Press. [Google Scholar](#)

Wang TD, Sakarinculu YA, Neild A, et al. (2013) Position accuracy of time-of-arrival based ranging using visible light with application in indoor localization systems. *Lightwave Technology Journal* 31(20): 3302–3308. [CrossRef](#) [Google Scholar](#)

Woo J, Kim YI, Lee JO, et al. (2006) Localization of mobile robot using particle filter. In: *the international joint conference on SICE-ICASE, Busan*, pp.3031–3034. [Google Scholar](#)

Xu R, Yu R, Sun G, et al. (2011) Whistle: synchronization-free TDMA for localization. In: *the 31st international conference on distributed computing systems*, Minnesota, pp.760–769. [Google Scholar](#)